First Results of Scintillator Readout With Silicon Photomultiplier

Deborah J. Herbert, Valeri Saveliev, Nicola Belcari, Nicola D'Ascenzo, Alberto Del Guerra, *Senior Member, IEEE*, and Alexei Golovin

***Abstract*—A new type of silicon device has been realized that has many properties comparable to, or better than, a conventional PMT (Photomultiplier Tube). This paper presents the first results of using these photodetectors in place of a PMT in the readout of scintillators for possible PET (Positron Emission Tomography) applications. This device, the Silicon Photomultiplier (SiPM), is effectively an avalanche photodiode operated in Geiger mode. In Geiger-mode detectors, a very large current signal is produced regardless of the size of the input, giving just logical rather than proportional information. However, the SiPM is subdivided into a large number (1440) of microcells that act as independent and virtually identical Geiger-mode photodiodes. The outputs of all these individual microcells are connected so that the total output signal is the sum of the signals from all of the microcells that were activated. In this way proportional information can be obtained. As a consequence of their design, these detectors have potentially very fast timing, high gain $(10^5 - 10^6)$ at low bias voltage ($\sim$50 V), a high quantum efficiency (35% at 500 nm), excellent single photoelectron resolution and are cheap to manufacture. Here we present results obtained with this new photodetector when used with pulsed LED and scintillator pixels.**

***Index Terms*—Photodetector, scintillator, SiPM, silicon photomultiplier.**

I. Introduction

The Metal-Resistor-Semiconductor (MRS) structure Silicon PhotoMultiplier (SiPM) is a new type of Geiger-mode avalanche photodiode that shows promise for use with scintillators [1]. They have recently been tested as possible detectors for the hadron calorimeter tiles for the TESLA next-generation linear collider [2]. This paper presents results from initial tests to characterize a SiPM test sample in terms of its general performance and for the readout of scintillators that are commonly used for PET.

The SiPM is a p-n junction diode that is biased above the breakdown voltage in order to create a Geiger avalanche. The resulting depletion region in this device is of the order of just 5 μm, with an avalanche region of around 1 μm. Such a thickness is sufficient for optical photon detection. The Geiger avalanche is passively quenched by a resistive load in series with the diode. In the MRS structure of this SiPM, the resistive load takes the form of a special technology layer deposited on the diode surface. By using the high-resistivity material SiC, the resistor element can be made small whilst providing adequate quenching. A semi-transparent metal contact layer on top of the quenching resistance forms the electrode. Such an MRS structure provides noiseless, high gain such that even a single optical photon can be easily detected and resolved.

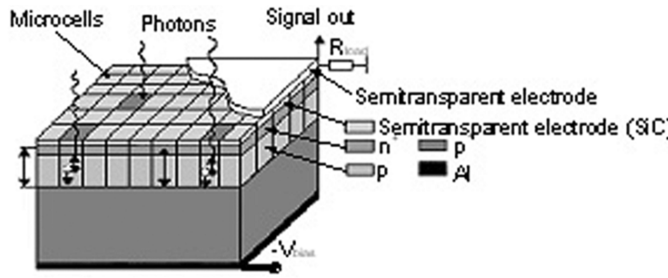

Fig. 1. Illustration of the MRS SiPM structure from CPTA, Moscow.

However, a normal Geiger-mode APD has the disadvantage that every photoelectron signal produced in the depletion region produces the same fixed amplitude output signal, the magnitude of which is determined by the quenching resistance. In this way a Geiger-mode APD performs as a digital counter, giving no information of the number of original photoelectrons produced and thus prohibiting the possibility of having proportional information for spectroscopy. Such GAPD devices have been studied elsewhere [3], [4] and are available commercially [5]. The MRS SiPM structure overcomes this inherent limitation by dividing the silicon-diode surface area into a large number of regions called microcells, each of which acts like an independent and identical Geiger-mode APD. This is achieved by forming the p-n junction as $\sim 20 \times 30$ μm^2 cells, separated by a gap of a few microns, which defines the detector structure, as shown in Fig. 1. Thus, the avalanche region is localized to each cell. If the outputs of all these microcells are summed together then the output signal is proportional to the number of microcells activated. In the MRS SiPM, the microcell signals are multiplexed by the common metal electrode contact layer. In this way, the MRS SiPM provides a large, proportional signal for low to moderate photon flux $(\mathrm{N_{photons}} < \mathrm{N_{cells}})$.

II. Materials and Methods

The MRS SiPM that was used in the measurements presented here was developed at CPTA (Center for Perspective Technology and Apparatus), Moscow. It has an area of 1×1 mm^2 and is composed of 1440 microcells, a close-up of which is

Manuscript received October 30, 2004.
D. J. Herbert is with INFN Pisa, Pisa I-56127, Italy (e-mail: herbert@df.unipi.it).
N. Belcari, N. D'Ascenzo, and A. Del Guerra is with Dipartimento di Fisica, University of Pisa, Pisa I-56127, Italy (e-mail: belcari@df.unipi.it; nicoladascenzo@yahoo.it; alberto.delguerra@df.unipi.it).
V. Saveliev and A. Golovin are with Obninsk State University of Nuclear Engineering, Studgorodok 1, 249040 Russia (e-mail: saveliev@mail.desy.de).
Digital Object Identifier 10.1109/TNS.2006.869848

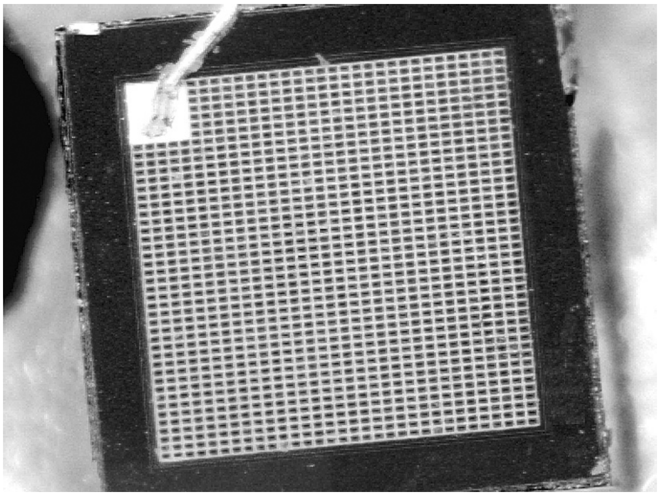

Fig. 2. Close-up of the SiPM surface; 1440 microcells covering a 1×1 mm^2 surface.

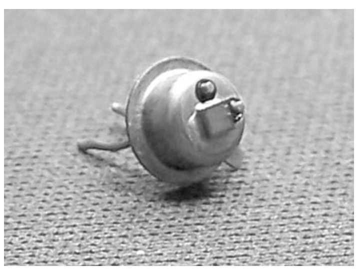

Fig. 3. SiPM test device from CPTA, Moscow.

shown in Fig. 2. A photo of the mounted test device is shown in Fig. 3. It is operated within the bias range of −48-−53 V. It should be noted that all measurements were made at room temperature; no cooling is required.

The SiPM bias was provided by a TTi QL564 high-precision voltage supply. The SiPM output signal, although already large from the avalanche amplification process, then entered a fast, charge-amplifier chip to better put the signal in the range of the CAEN V785 QDC (charge integrating ADC). The resulting data was then sent to a PC and acquired, displayed and analyzed using a custom LabView program.

Initial characterizations of the SiPM were carried out using pulsed LED's, driven by a Philips PM5715 pulse generator. The QDC requires a gate signal for acquisition that was also generated by the pulse generator. Measurements of scintillation spectra were made by coupling the SiPM, in turn, to three types of inorganic scintillator; LSO, which is currently the optimum choice for most PET applications, and BGO and CsI(Tl), which were chosen for study due to their longer wavelength emissions. The BGO and LSO scintillators were $1.5 \times 1.5 \times 12$ mm^3 in size whilst the CsI(Tl) crystal was $1 \times 1 \times 1$ cm^3.

A. Gain

By pulsing the LED at a very low light level, the SiPM is able to clearly resolve single photoelectron peaks. The LED pulse width was set at 20 ns FWHM (the minimum for our pulser); a narrow pulse width is preferable in order to have the shortest possible QDC gate (50 ns), integrating the minimum amount of noise in order to see the best resolution peaks. The single photoelectron separation in the resulting spectrum, obtained by fitting the peaks with Gaussian functions, gives the gain of the device. The gain is a function of bias, since the SiPM charge signal is essentially current limited by the resistive layer. Therefore, using a larger voltage will permit a larger current to flow. The gain was measured for the full range of bias values.

B. Dark Count Rate

Due to the very high gain of the SiPM, the standard photodiode noise considerations are not applicable. However, there remains a significant contribution from dark counts that are due to thermally-generated electrons in the depletion region. These cause an avalanche and generate a signal that is indistinguishable from that produced by a "signal" photoelectron. Therefore, these events can be thought of as noise at the photoelectron level. The dark count rate increases with temperature, detector volume and bias; Increasing the bias, and therefore the field strength at the junction, increases the probability of thermal generation and collection of electrons from outside the depletion region.

Such signals can be easily seen in the absence of any incident light. To measure the dark count rate, the SiPM output was sent to a CAEN N840 threshold discriminator and the generated triggers counted with a CAEN N1145 scalar unit. The rate was calculated for different SiPM bias voltages.

C. Detection Efficiency as a Function of Bias

The overall detection efficiency of the SiPM is a combination of three factors; the intrinsic quantum efficiency of the silicon, the geometrical active area and the probability of initiating an avalanche. The first two components are fixed for a particular device but the third varies as a function of the bias voltage applied. This can be explained by the fact that increasing the bias increases the field strength, leading to a more efficient electron collection. This leads to the detection of more photons interacting near the top surface of the silicon. Measurements of the absolute detected quantum efficiency (DQE) as a function of wavelength of this device have been made at CERN [6]. Here we make a comparative study of how the DQE varies for different bias voltages for a fixed wavelength. This was achieved using a pulsed, red LED of a fixed light level, and measuring the average signal level detected by the SiPM for different biases. The LED pulse width was again 20 ns FWHM, at a relatively low light level $(\mathrm{N_{photons}} \ll \mathrm{N_{cells}})$. The average detected signal level was then calculated from the centroid of each spectrum measured by the QDC in terms of the detected number of photoelectrons $(\mathrm{N_{pe}})$.

D. Recovery Time

In order to measure the recovery time of the SiPM setup, double pulses from the pulsed LED with different temporal delay were used. The LED pulse width was again 20 ns FWHM with a signal level of about 20 photoelectrons.

E. Scintillation Spectra

Well polished LSO and BGO scintillation pixels of $1.5 \times 1.5 \times 12$ mm^3 were wrapped in several layers of white

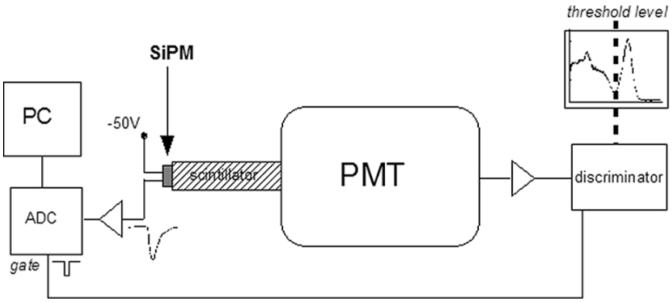

Fig. 4. Setup showing how the SiPM scintillation spectra were obtained. The scintillator, as well as being coupled to the SiPM, is also coupled at the opposite end to a PMT. This PMT signal is used to create the trigger for the ADC when a photopeak event is detected.

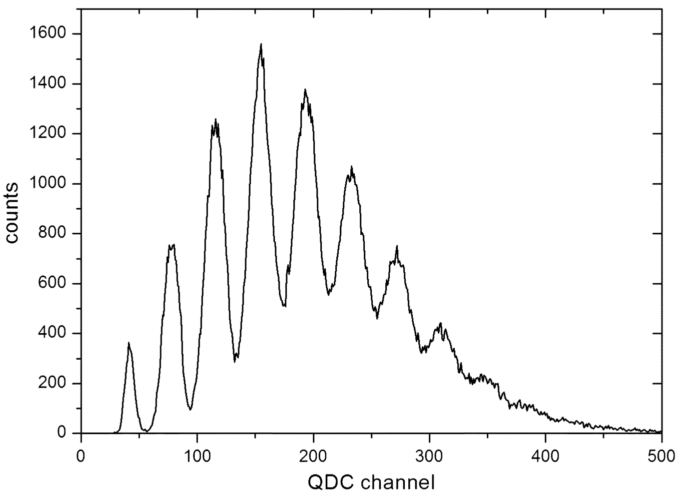

Fig. 5. SiPM single photoelectron spectrum from a low light level LED.

Teflon tape and air-coupled, centrally, to the SiPM. The crystal was illuminated from the side by a ^{22}Na source. A gate signal for the QDC was necessary, which was made by placing a PMT at the opposite end of the crystal to view a small portion of the light signal, and thus provide a trigger. The gate signal for LSO was 120 ns in width, whilst that for BGO was 300 ns. The experimental arrangement can be seen in Fig. 4. The face of the crystal coupled to the PMT was actually covered with a couple of layers of Teflon tape in order to allow just enough light to pass to generate a trigger. The trigger threshold for the PMT was set just below the 511 keV photopeak level. Therefore, the resulting SiPM spectrum represents just photopeak events. This method was used in order to find the photopeak centre in the absence of any photopeak resolution due to the low expected photon statistics. From the position of the centre of this peak, we determined the average $\mathrm{N_{pe}}$ for a 511 keV deposit.

III. Results

A. Gain

A typical single photoelectron spectrum is shown in Fig. 5. Such well-resolved singles peaks are possible due to the large signal-to-noise ratio of the SiPM. The width of the single photoelectron peaks is a combination of the system noise, as represented by the pedestal, the statistical variation on the number of electrons produced per avalanche, which is very small, and

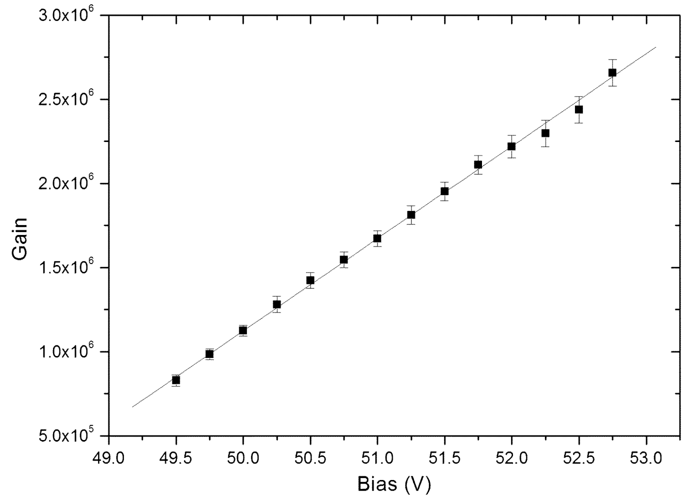

Fig. 6. SiPM gain as a function of bias voltage, with a linear fit.

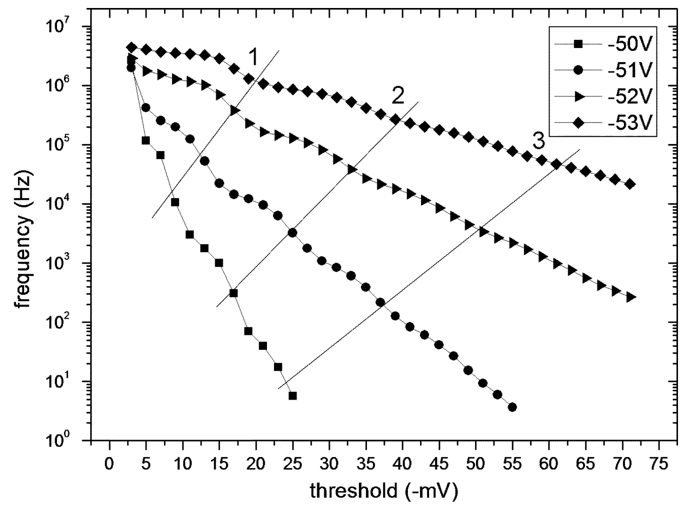

Fig. 7. SiPM dark count rate for different biases and thresholds. The regions corresponding to different numbers of photoelectrons are indicated.

the variations in the response of the different microcells. Any device instability would also be indicated by decreased resolution. Each QDC channel is equal to 0.1 pC and from this the gain is calculated and is shown for each bias value in Fig. 6. The gain was found to be linear and in the range of 8×10^5 and 3×10^6 between the bias values of 49.5–53 V.

B. Dark Count Rate

The measured dark count rates for different biases at different thresholds are shown in Fig. 7. The 'bumps' seen in the graphs are due to the individual photoelectrons. The gain increase at different biases is also evident from the spacing of the 'bumps'. The frequency of the thermal events can be seen to increase radically between a bias value of 50–53 V. The dark count rate for a threshold at the single photoelectron level varies between 20 kHz and 1 MHz for bias values of 50–53 V. At a level of three photoelectrons, there are just a few counts a second at 50 V but still 50 kHz at 53 V. But for an ADC gate of 120 ns, which is that required to fully integrate a signal from LSO, the probability of integrating dark counts in that period is negligible, even at

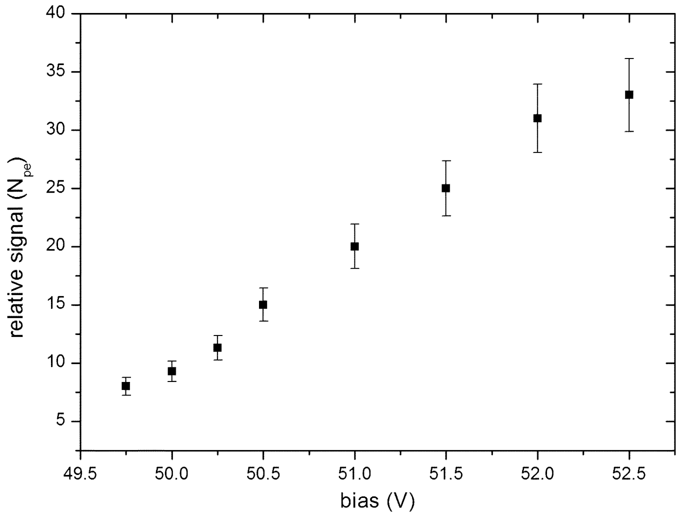

Fig. 8. Relative signal size for a fixed LED light level, showing the increase of the DQE as a function of bias voltage.

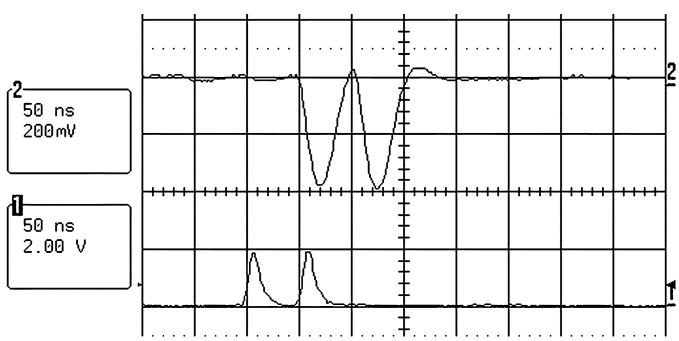

Fig. 9. Fully resolved signals from the SiPM (top trace), and the LED input pulses with 50 ns delay (bottom trace).

53 V. Assuming that the quantum efficiency of the SiPM can be improved, the numbers of photoelectrons that we expect in nuclear medicine applications with inorganic scintillators should be sufficiently large, such that a threshold of several photoelectrons should be no problem.

C. Detection Efficiency as a Function of Bias

Fig. 8 shows the increase in the average detected signal, in terms of the $\mathrm{N_{pe}}$, at different bias values for a fixed light level. The detection efficiency was found to increase significantly, with signals increasing by a factor of four between the bias values of 49.5–53 V. Since the overall DQE was found to be low for this SiPM [6], particularly around the emission wavelengths of LSO, it is be vital to maximize the DQE in this way; this implies that the highest bias value possible should be used.

D. Recovery Time

Fig. 9 shows the oscilloscope capture of two SiPM signals that are just temporally separated (upper trace). The separation of the input pulses to the LED was 50 ns (bottom trace). In fact this "recovery time" is really a worst-case scenario. The time response in these tests was dominated by the >20 ns LED pulse width used. In fact, the amplitude and timing of these pulses is representative of the LSO signals observed in Fig. 10. What

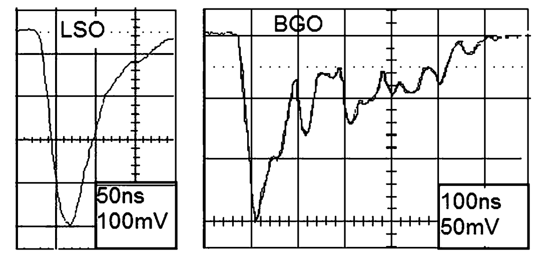

Fig. 10. Oscilloscope captures of 511 keV photopeak pulses for LSO and BGO. Note the different scales. Although the signals consist of approximately the same number of photoelectrons, the BGO signal is emitted over a much longer period and hence the statistical fluctuations can be seen.

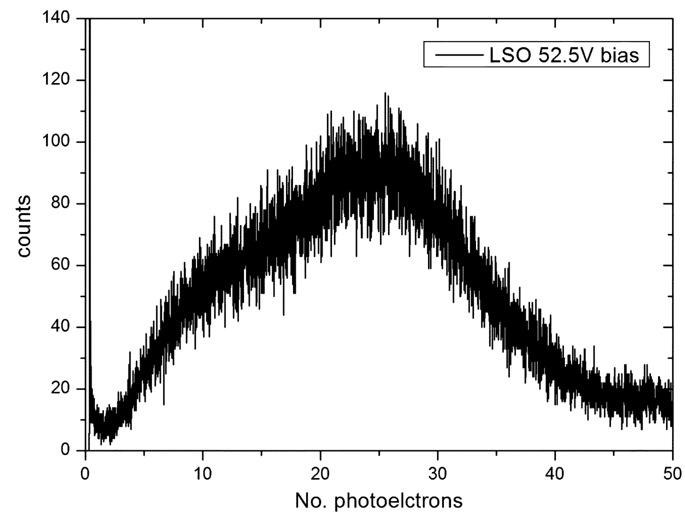

Fig. 11. LSO 511 keV photopeak spectrum.

we can conclude from this is that at worst, the complete recovery time is 50 ns—more than adequate for scintillator applications, although previous studies have shown intrinsic timing of <100 ps [1], [2]. Importantly, this device does not have the long recovery time, of several tens of microseconds, associated with other types of Geiger-mode APD [3]. It should be noted that only by saturating the SiPM can the true recovery time be determined, which is a subject for future study.

E. Scintillation Spectra

Figs. 11 and 12 show the pulse height spectra and Fig. 10 the oscilloscope captures for LSO and BGO. Due to the method of thresholding that was used virtually all of the Compton scattered events were rejected and the observed "peak" consists almost entirely of 511 keV photopeak events, with a small underlying continuum of 1274 keV events which were rejected. In the case of both LSO and BGO, the centre of this "peak" is around 25 p.e. This signal level is obviously significantly lower than what would be expected from these scintillators at this gamma-ray energy. Using the QE values measured in [6] and convolving them with the emission spectra of the scintillators, it can be seen that the average DQE is very low. The values are given in Table I along with the absolute scintillation yields of each scintillator [7]. The product of these numbers explains why we see a virtually identical absolute scintillation yield for BGO and LSO. It also implies a light collection efficiency (LCE) as

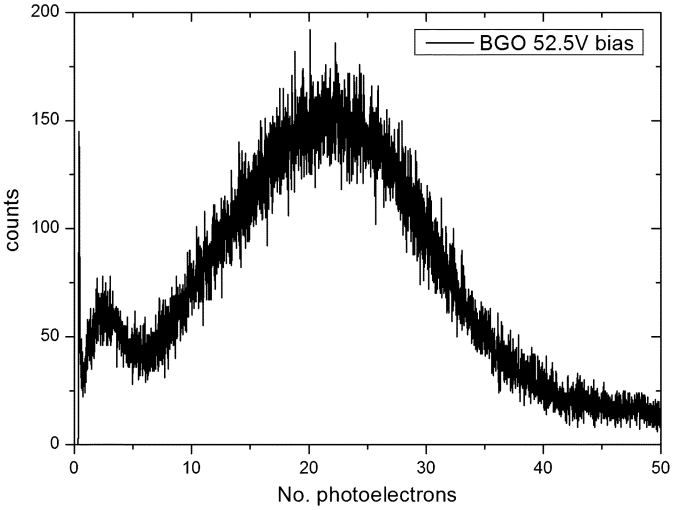

Fig. 12. BGO 511 keV photopeak spectrum.

TABLE I
AVERAGE QUANTUM EFFICIENCY OF THE SIPM FOR VARIOUS SCINTILLATORS AND THEIR ABSOLUTE SCINTILLATION YIELD

	Average QE (%)	Light yield (Ph/MeV)
LSO	2.5	25 000
BGO	9	8 200
CsI(Tl)	14	65 000

little as 7%. Obviously, the crystal size of 1.5×1.5 mm^2 isn't well adapted to the 1×1 mm^2 active area of the detector, but was the smallest available at the time of these measurements. Work is currently in progress with 1×1 mm^2 pixel crystals of the same materials. In addition, the air coupling contributes to the poor LCE.

The oscilloscope captures show typical pulses for LSO and BGO (Note that both time and amplitude scales differ in the two plots). It is interesting, that despite the fact that both pulses consist of 25 p.e, they have very different forms. This is because BGO produces the 25 photoelectrons over a period of time several times longer than that of LSO. So instead of being smooth like the LSO, individual photon structure within the pulse can be observed.

A very large signal was observed on the oscilloscope for CsI(Tl), as shown in Fig. 13. Its very long decay time makes it unsuitable for PET and difficult to acquire with our QDC without also integrating a large amount of noise (a 3 μs gate would be required). Note that although the signal does not have a very large amplitude, it has a long decay time. We have estimated this pulse to correspond to around 500 p.e, which given the hugely inappropriate crystal geometry and coupling is significant. This large signal is a consequence of CsI(Tl)'s large scintillation yield and also its emission spectrum, which is predominantly in the red (550 nm) where the SiPM has a higher QE.

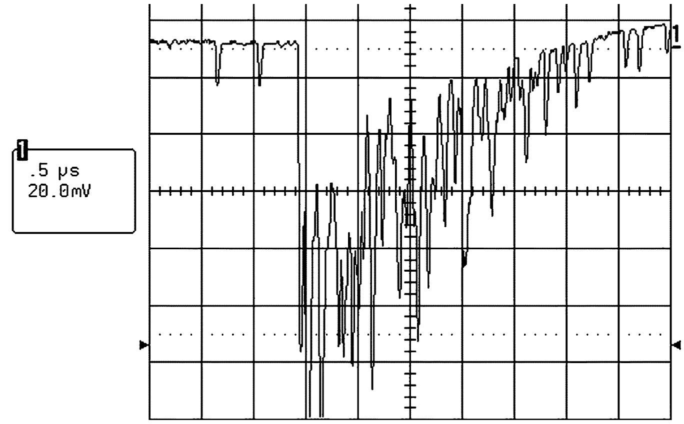

Fig. 13. Oscilloscope capture of a 511 keV photopeak event in CsI(Tl).

IV. SUMMARY

The preliminary studies we have made of the MRS SiPM sample have demonstrated a very promising photodetector that is stable and rugged, has excellent single photoelectron resolution, fast recovery time and a high gain at low bias voltage. No problems or failures were encountered during the several months in which this sample was tested. Its dimensions are ideal for forming high-resolution matrices for PET or other scintillator-imaging applications. The fabrication is fairly simple and does not require special high-resistivity silicon, therefore having the potential to be a low-cost detector solution. There is no requirement for special, low-noise electronics since the gain is of the order of $8 \times 10^5 - 3 \times 10^6$ between the bias values of 49.5–53 V. Even at maximum gain, a threshold of 3 p.e keeps the dark count rate to around 50 kHz. The gain was monitored using the single photoelectron peaks, at fixed settings, over a period of several months in a range of laboratory temperatures. The gain fluctuations at different times, during these months in which it was tested, were found to be small (standard deviation $<1\%$). These could be attributed to changes in ambient temperature, instabilities in the bias supply and measurement errors.

The disappointment with this SiPM was that the quantum efficiency for our sample was found to be very low, averaging only 2.5% over the emission spectrum of LSO. When the measurements were made with scintillator light signals, the measured number of photoelectrons was significantly less than had been expected. With a traditional PMT we would typically expect a signal of >1000 p.e with such a scintillator at 511 keV. Although a small amount of light is lost to the PMT to make the trigger in our set up, this was kept to a minimum by keeping layers of Teflon between the scintillator and PMT. Even taking into account the low average DQE over the LSO spectrum, this leads to an exceptionally small LCE. However, considering the poor (air) coupling and inappropriate geometry it is possible. Measurements using 1×1 mm^2 pixels with improved optical coupling will be made shortly, as well as studies of the expected LCE made from measurements of the pixels on a standard PMT.

Our work in studying the SiPM with a fixed level light source demonstrated that by increasing the bias voltage a significant increase in the DQE can be obtained. Although, of course, the overall DQE remains low, it seems reasonable to assume that a higher bias voltage should be used. However, such a decision has to be weighed against the accompanying disadvantages. As well as improved detection efficiency and higher gain, a high bias also increases the dark rate.

Our main priority for future work will concentrate on improving the sensitivity of the devices in the blue region. At Pisa we have now developed dedicated fast readout and have fast-pulsed light sources. Measurements with this new setup will soon commence and will permit a proper investigation of the timing behavior of these detectors. Once the SiPM structure has been optimized, we then have the intention to build matrices of the devices. This is difficult as the signal is currently collected from the top of the device (the illumination side). However, ways to overcome these problems are currently in development.

REFERENCES

[1] V. Saveliev and V. Golovin, "Silicon avalanche photodiodes on the base of metal-resistor-semiconductor (MRS) structures," *Nucl. Instr. Meth.*, vol. A442, pp. 223–229, 2000.

[2] V. Golovin and V. Saveliev, "Novel type of avalanche photodetector with Geiger mode operation," *Nucl. Instr. Meth*, vol. A518, pp. 560–565, 2004.

[3] S. Vasile, P. Gothoskar, D. Sdrulla, and R. Farrell, "Photon detection with high gain avalanche photodiode arrays," *IEEE Trans. Nucl. Sci.*, vol. 45, no. 720, pp. 720–723, Jun. 1998.

[4] J. C. Jackson, D. Phelan, A. P. Morrison, R. M. Redfern, and A. Mathewson, "Characterization of geiger mode avalanche photodiodes for fluorescence decay measurements," in *Proc. SPIE*, vol. 4650–07, 2002, pp. 55–56.

[5] [Online]. Available: http://www.apeakinc.com

[6] Y. Musienko, "Advances in avalanche photodiodes," presented at the *Innovative Detectors Supercolliders*, Erice, Italy, Sep. 2003.

[7] G. Knoll, *Radiation Detection and Measurement*, 3rd ed. New York: Wiley, 2000, p. 235.